

# Ultraeffective ZnS Nanocrystals Sorbent for Mercury(II) Removal Based on Size-Dependent Cation Exchange

Zan Qu,<sup>†</sup> Lili Yan,<sup>‡</sup> Liang Li,<sup>\*,†</sup> Jianfang Xu,<sup>†</sup> Mingming Liu,<sup>†</sup> Zhichun Li,<sup>†</sup> and Naiqiang Yan<sup>\*,†</sup>

<sup>†</sup>School of Environmental Science and Engineering, Shanghai Jiao Tong University, Shanghai 200240, China

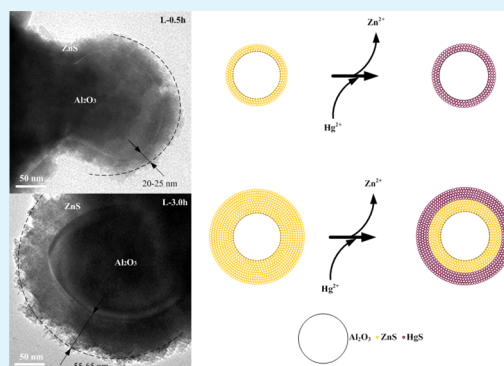
<sup>‡</sup>School of Agriculture and Biology, Shanghai Jiao Tong University, Shanghai 200240, China

## Supporting Information

**ABSTRACT:** We report a novel nanocrystals (NCs) sorbent, which shows an extraordinary adsorption capacity to aqueous  $\text{Hg}^{2+}$  based on cation exchange and allows for the utmost removal of mercury from water. The NCs sorbent was synthesized by direct coating ZnS NCs on the surface of the  $\alpha\text{-Al}_2\text{O}_3$  nanoparticles. The as-prepared ZnS NCs sorbent can efficiently remove over 99.9%  $\text{Hg}^{2+}$  in 1 min, and lower the  $\text{Hg}^{2+}$  concentration from 297.5 mg/L (ppm) to below 1.0  $\mu\text{g/L}$  (ppb) within 5 min. The saturated adsorption capacity of ZnS NCs for  $\text{Hg}^{2+}$  is about 2000 mg/g, which is close to the theoretic saturated adsorption capacity. The mechanism of  $\text{Hg}^{2+}$  removal by ZnS NCs sorbent, the influences of pH value and other cations on  $\text{Hg}^{2+}$  removal were investigated, respectively. Meanwhile, it is found the size-dependent cation exchange plays a critical role in the removal of  $\text{Hg}^{2+}$  by ZnS NCs. Small size ZnS NCs shows better performance than the big size ZnS NCs in the adsorption capacity and adsorption rate for  $\text{Hg}^{2+}$ .

Furthermore, the mercury adsorbed by the ZnS NCs sorbent is readily recycled by extraction with aqueous sodium sulfide.

**KEYWORDS:** nanocrystals, mercury removal, cation exchange, size-dependent, ZnS sorbents



## 1. INTRODUCTION

Mercury is a highly toxic and bioaccumulative heavy metal that could cause serious human health problems and has been an important concern for decades.<sup>1</sup> With the Minamata Convention on Mercury, at which an issued global treaty for the control of the worldwide mercury pollution was reached after negotiation by delegates from over 140 countries in 2013,<sup>2</sup> it becomes more urgent to reduce the mercury emission. Industrial wastewater is one of the major ways mercury pollutants enter the environment; the removal of mercury from wastewater is very important accordingly.<sup>3,4</sup> Although, how to efficiently remove the mercury from industrial wastewater is still very challenging.<sup>5</sup> The traditional mercury removal technologies include amalgamation, membrane separation, adsorption, etc.<sup>6–9</sup> However, the mercury removal efficiency of these technologies is still not satisfied yet. Therefore, it is significant to develop a more efficient mercury removal technique.

Semiconductor nanocrystals (NCs) are of great interest for technical applications such as biolabeling, lightening, display technology and solar energy conversion due to their unique properties, and their synthetic chemistry was extensively studied and a vast amount of synthetic procedures of NCs have been developed in the past decade.<sup>10–12</sup> Among these procedures, cation exchange has become a convenient synthetic tool to allow nanomaterials chemists to achieve morphologies, shapes and structures that may be difficult to obtain by conventional synthesis.<sup>13–16</sup> For example, an easily synthesized

nanostructure such as CdS NCs is first synthesized as a template, and then the reactants contain  $\text{Pb}^{2+}$  or  $\text{Hg}^{2+}$  were added, the  $\text{Cd}^{2+}$  of CdS NCs will be easily and quickly exchanged by  $\text{Pb}^{2+}$  or  $\text{Hg}^{2+}$ .<sup>11</sup> The reaction time of cation exchange in the NCs is much shorter ( $\ll 1$  s) than that of the related systems of large size (e.g., 10 h for 100 nm CdS wire and weeks for bulk crystals),<sup>16</sup> likely due to enhanced surface access and lower activation barriers to diffusing ions. These features make NCs potentially suitable as an effective heavy metal ions exchanger and remover. Such an application is based on NCs' intrinsic cation exchange properties and will open a new window for the application of NCs. For example, low toxic  $\text{Cu}_2\text{X}$  ( $\text{X} = \text{S}, \text{Se}, \text{Te}$ ) NCs can be readily transformed to  $\text{HgX}$  and  $\text{PbX}$  ( $\text{X} = \text{S}, \text{Se}, \text{Te}$ ) NCs through cation exchange reaction with  $\text{Hg}^{2+}$  and  $\text{Pb}^{2+}$  under ambient conditions,<sup>11</sup> which could be utilized to remove the heavy metal ions, such as  $\text{Hg}^{2+}$ , from wastewater. However, to date, few research efforts have investigated whether the cation exchange of NCs can be directly useful to remediate mercury contaminated water. Moreover, there have been few studies about how the size of NCs affects the cation exchange speed and degree, which is critical for its application in heavy metal ions removal. Therefore, this paper developed a novel ZnS NCs sorbent and tested its performance in  $\text{Hg}^{2+}$  removal from water.

Received: July 24, 2014

Accepted: September 26, 2014

Published: October 9, 2014

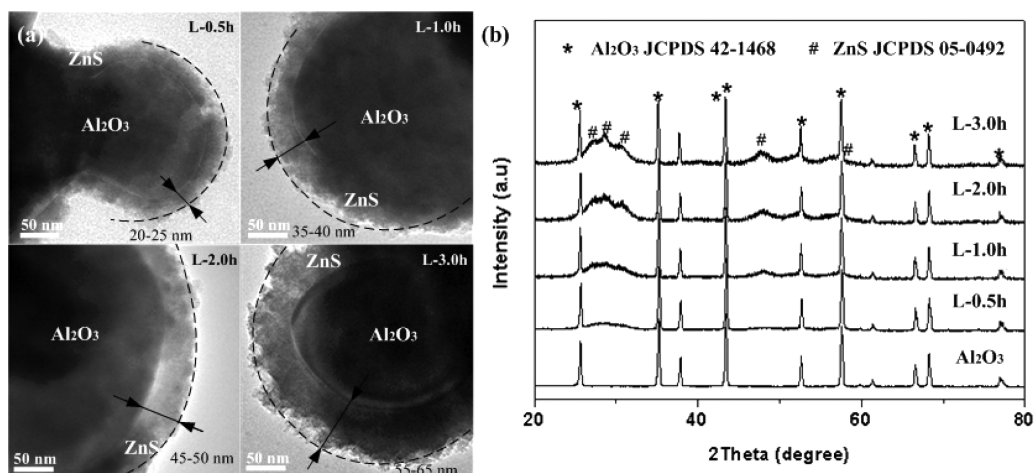


**Figure 1.** TEM images (a) and XRD patterns (b) of ZnS NCs sorbents prepared at 180 °C for different reaction times.

Meanwhile, the influence of NCs sizes on the removal of  $\text{Hg}^{2+}$  was also investigated.

## 2. EXPERIMENTAL METHODS

**2.1. Materials.**  $\alpha\text{-Al}_2\text{O}_3$  (99.99%, 200 nm), mercury chloride (>99%), zinc chloride (>99%), lead nitrate (>99%), cadmium chloride (>99%), nickel nitrate (>99%), cobalt nitrate (>99%), copper sulfate (>99%), calcium chloride (>99%), chromium chloride (>99%), hexahydrate (>99%), sodium sulfide (>99%), ethylene glycol (>99%), 1-butylamine (>99%) and triethylene glycol (>99%) were provided by Aladdin Chemical (Shanghai, China). Thiourea (99%) was provided by Sigma-Aldrich (St. Louis, MO).

**2.2. Synthesis of ZnS NCs Sorbents.** To easily separate the ZnS NCs sorbent from the water after the mercury adsorption experiment,  $\alpha\text{-Al}_2\text{O}_3$  (200 nm) was chosen as the carrier of ZnS NCs sorbent in this research. 2 mmol  $\alpha\text{-Al}_2\text{O}_3$  was mixed with 2 mmol  $\text{ZnCl}_2$  and 200 mL of ethylene glycol in a 500 mL three-neck flask equipped with a condenser. A mixture of 3 mmol thiourea dissolved in 10 mL of 1-butylamine and 40 mL of ethylene glycol is injected continuously into the reaction solution over 3 h by a syringe pump at 180 °C. The surface of the  $\text{Al}_2\text{O}_3$  is covered by hydroxyl groups in the glycol solution,<sup>17,18</sup> which will adsorb  $\text{Zn}^{2+}$  that subsequently react with  $\text{S}^{2-}$  from decomposition of thiourea to form ZnS nanoparticles on  $\text{Al}_2\text{O}_3$ . Four ZnS NCs sorbents were sampled from the reaction solution at 0.5, 1.0, 2.0 and 3.0 h, which were marked as L-0.5h, L-1.0h, L-2.0h and L-3.0h, respectively. To synthesize bigger ZnS NCs, the reaction temperature was increased to 270 °C and the reaction solvent (ethylene glycol) was replaced by triethylene glycol, which has a higher boil temperature (285 °C). The ZnS NCs synthesized at higher temperatures were marked as H-0.5h, H-1.0h, H-2.0h and H-3.0h, respectively. It deserves attention that the cost of synthesizing ZnS NCs by this way is much lower than the conventional hot injection technology in a noncoordinating organic solvent.

**2.3. Characterizations.** Morphology observations and energy dispersive X-ray (EDX) analysis of the samples were conducted with high-resolution transmission electron microscopy (HRTEM, JEOL 2010, Tokyo, Japan). X-ray diffraction (XRD) patterns were recorded by a Shimadzu XRD-6000. The surface area of ZnS NCs sorbents was detected by a surface area and pore size analyzer (Quantachrome Instruments NOVA 2200e, Boynton Beach, FL).

**2.4. Adsorption Experiments.** Because the Hg contamination in industrial wastewater exists primarily as  $\text{Hg}^{2+}$ ,<sup>19</sup>  $\text{HgCl}_2$  was chosen as the representative mercury pollutant in this research. All batch sorption experiments were performed by mixing a certain amount of ZnS NCs sorbent into a predetermined concentration of  $\text{HgCl}_2$  solution with stirring (400 r/min) at room temperature. The solution was sampled and filtrated by filter (pore size: 220 nm) at different reaction times. Meanwhile, the solution samples were analyzed by a

mercury analyzer (RA915, St. Petersburg, Russia) and continuum source atomic absorption spectrometry (ContrAA 700, Jena, Germany).

## 3. RESULTS AND DISCUSSION

**3.1. Characterization.** Figure 1a is the transmission electron microscopy (TEM) images of ZnS NCs sorbents prepared at 180 °C for different synthesis times (0.5, 1.0, 2.0 and 3.0 h), which were marked as L-0.5h, L-1.0h, L-2.0h and L-3.0h, respectively. The  $\alpha\text{-Al}_2\text{O}_3$  nanoparticles appear as aggregates, and we observe that all  $\alpha\text{-Al}_2\text{O}_3$  nanoparticles in the product have been fully coated with ZnS NCs layers (Figure S1, Supporting Information). The ZnS NCs coating layers follow the shape of the  $\alpha\text{-Al}_2\text{O}_3$  template with an average thickness of about 20–25 nm for the sample taken at 0.5 h, and become thicker and thicker with the synthesis time increased from 0.5 to 3.0 h. The fine control of the ZnS NCs layer thickness was achieved by continuous injection with a syringe pump that was commonly used to avoid self-nucleation during shell growth of core/shell NCs,<sup>20,21</sup> which is the reason why we did not find free ZnS NCs formed in the above samples. To know the change in surface area of the ZnS NCs sorbent with synthesis time, the surface area of L-0.5h, L-1.0h, L-2.0h and L-3.0h was tested and the results are about 15.3, 13.8, 10.6 and 9.5  $\text{m}^2/\text{g}$ , respectively. It seems the increasing thickness of the ZnS shell will decrease the surface area of ZnS NCs sorbents.

The results of powder X-ray diffraction (XRD, Figure 1b) further identify the samples are mixtures of wurtzite ZnS NCs and  $\alpha\text{-Al}_2\text{O}_3$ ; those sharp peaks are from  $\alpha\text{-Al}_2\text{O}_3$  nanoparticles, and the broad and weak peaks are from wurtzite ZnS NCs. With the synthesis time changing from 0 to 3.0 h, the XRD peaks of ZnS NCs became stronger and stronger, confirming more and more ZnS NCs formed with the reaction time evolution. Chemical analysis using energy dispersive X-ray spectrometry (EDX, Figure S2, Supporting Information) indicates the presence of Zn, S, Al and O in the sorbents. The atomic ratio of Zn to S is near to 1:1 and the ZnS/ $\text{Al}_2\text{O}_3$  mole ratios are close to 0.24:1, 0.59:1, 0.93:1 and 1:1 for the samples taken at 0.5, 1.0, 2.0 and 3.0 h, respectively, which are close to the theoretical numbers. It indicates the reaction between  $\text{Zn}^{2+}$  and thiourea is quite complete. As shown with HRTEM (Figure S3, Supporting Information), the coating layer is composed of ZnS NCs around 4–5 nm, which is consistent with those numbers calculated from the XRD results

by the Scherrer Equation. No significant sizes difference was observed for the four samples synthesized at 180 °C.

**3.2. Adsorption Kinetics.** To evaluate the suitability of ZnS NCs sorbent for removal of  $\text{Hg}^{2+}$  from wastewater, the mercury removal performance of ZnS NCs sorbent under different initial  $\text{Hg}^{2+}$  concentrations range from 297.5 mg/L (ppm) to 0.3 mg/L (ppm) was investigated by using the L-0.5h sample (Figure 2). 100 mg of ZnS NCs sorbent was added into

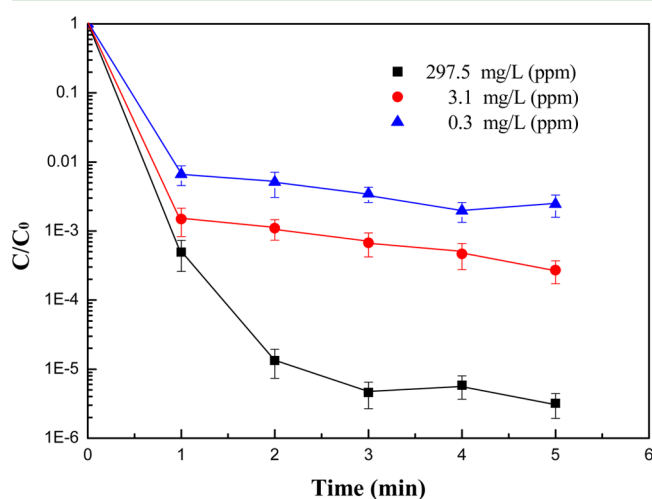


**Figure 2.** Ratio of  $\text{Hg}^{2+}$  concentration at different treating time to initial  $\text{Hg}^{2+}$  concentration ( $C/C_0$ ) as a function of time for mercury removal by ZnS NCs sorbent (L-0.5h). 100 mg of ZnS NCs sorbent was added into 50 mL of  $\text{HgCl}_2$  solution with stirring (400 r/min). The initial  $\text{Hg}^{2+}$  concentrations range from 297.5 mg/L (ppm) to 0.3 mg/L (ppm). The pH value of  $\text{HgCl}_2$  solution (297.5 mg/L) is about 5.5.

50 mL of  $\text{HgCl}_2$  solution with stirring (400 r/min). On the basis of the adsorption experiment results in Table 1 and Figure

**Table 1. Initial and Final Concentrations of  $\text{Hg}^{2+}$  after Adsorption**

initial concentration (mg/L)	final concentration ( $\mu\text{g/L}$ )	reaction time (min)
297.5	0.9	5
3.1	0.8	5
0.3	0.7	5

2, the ZnS NCs sorbent (L-0.5h) can efficiently remove over 99.9%  $\text{Hg}^{2+}$  in 1 min, and lower the  $\text{Hg}^{2+}$  concentration from 297.5 mg/L (ppm) to below 1.0  $\mu\text{g/L}$  (ppb) within 5 min. For the solutions with lower initial  $\text{Hg}^{2+}$  concentrations, their  $\text{Hg}^{2+}$  concentrations also decreased quickly to below 1.0 ppb with treatment for 5 min. Such final concentrations are lower than of World Health Organization guidelines (6 ppb  $\text{Hg}$ ),<sup>22</sup> even lower than the maximum contaminant mercury level in drinking water allowed in the United States (2 ppb)<sup>23</sup> and drinking water standards of the European Union (1 ppb).<sup>24</sup> Therefore, it is efficient enough for the mercury removal from industrial wastewater.

**3.3. Mechanism of Mercury Removal by ZnS NCs Sorbent.** It was found that the color of the ZnS NCs sorbent turned to yellow quickly, and to brown a few minutes after it was mixed with  $\text{Hg}^{2+}$  containing water (Figure S4, Supporting Information). According to Figure 2, we know that about 99.9%

$\text{Hg}^{2+}$  was removed by the ZnS NCs sorbent in 1 min. If all of the  $\text{Hg}^{2+}$  was removed by ZnS NCs sorbent and converted to  $\text{HgS}$  in 1 min based on cation exchange, the color of the ZnS NCs sorbent should also turn to black in 1 min, which is different from what was observed in the reaction process. Obviously, the reaction between  $\text{Hg}^{2+}$  and ZnS NCs is not a simple cation exchange reaction. To investigate the mechanism of the reaction between  $\text{Hg}^{2+}$  and ZnS NCs, 100 mg of ZnS NCs sorbent (L-0.5h) was added into 50 mL of  $\text{HgCl}_2$  solution (1.8 mmol/L) with stirring (400 r/min), and the  $\text{Hg}^{2+}$  and  $\text{Zn}^{2+}$  concentrations of the sample during the reaction were analyzed, which are shown in Figure 3.

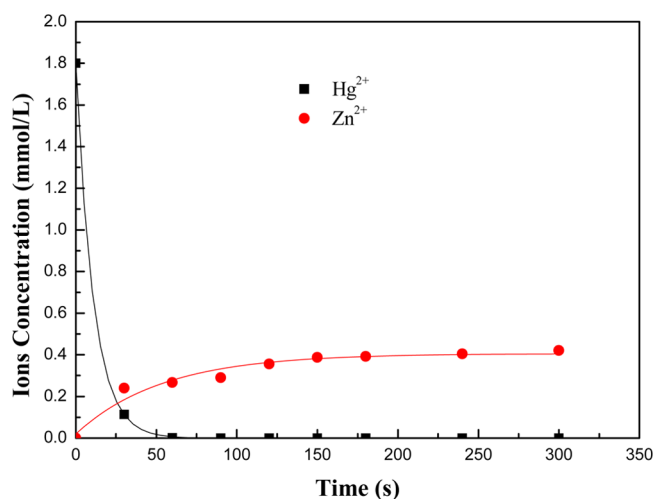


**Figure 3.**  $\text{Hg}^{2+}$  and  $\text{Zn}^{2+}$  concentrations of solution in the mercury removal process. 100 mg of ZnS NCs sorbent (L-0.5h) was added into 50 mL of  $\text{HgCl}_2$  solution ( $\text{Hg}^{2+}$  concentration: 1.8 mmol/L) with stirring (400 r/min). The pH value of the  $\text{HgCl}_2$  solution (1.8 mmol/L) is about 5.7.

From Figure 3, it can be seen that the  $\text{Hg}^{2+}$  concentration decreased quickly; about 99.9%  $\text{Hg}^{2+}$  is removed by the ZnS NCs sorbent in 60 s. However, the  $\text{Zn}^{2+}$  concentration increased slowly. The amount of ZnS NCs used in this experiment is much larger than that of  $\text{Hg}^{2+}$ . If the  $\text{Hg}^{2+}$  is totally exchanged by  $\text{Zn}^{2+}$  based on cation exchange, the  $\text{Zn}^{2+}$  concentration should increase to 1.8 mmol/L in 60 s. However, the  $\text{Zn}^{2+}$  concentration is about 0.4 mmol/L even when the reaction time is 300 s. Obviously, only part of  $\text{Hg}^{2+}$  is removed through cation exchange, the other part of  $\text{Hg}^{2+}$  is possibly adsorbed by the surface of ZnS NCs sorbent at 60 s, which is similar as the previous reports using NCs as a heavy metal ions sensor, where heavy ions tended to be adsorbed on the surface of NCs by ligands or  $\text{S}^{2-}$ .<sup>25,26</sup> However, the  $\text{Zn}^{2+}$  concentration reached 1.8 mmol/L after 24 h of reaction, which means all of the  $\text{Hg}^{2+}$  will finally enter the lattice of the ZnS and exchange  $\text{Zn}^{2+}$  out.

From the powder X-ray diffraction (XRD, Figure 4) of ZnS NCs sorbent (L-3.0h) before reaction and after 20 min of reaction, we see that there are two new peaks at about 22.4° and 34.6°, which are the characteristic peaks of  $\text{HgZnS}$ . It indicates the cation exchange really happens on ZnS NCs, where  $\text{Hg}^{2+}$  enters the lattice of the ZnS and forms a  $\text{HgZnS}$  alloy structure. Therefore, there may be two possible reaction pathways for  $\text{Hg}^{2+}$  removal by ZnS NCs, which could be deduced as follows. In pathway 1, the  $\text{Hg}^{2+}$  was first adsorbed by ZnS NCs and formed adsorptive  $x\text{Hg}\cdot\text{ZnS}_{(\text{ad})}$ . Then the



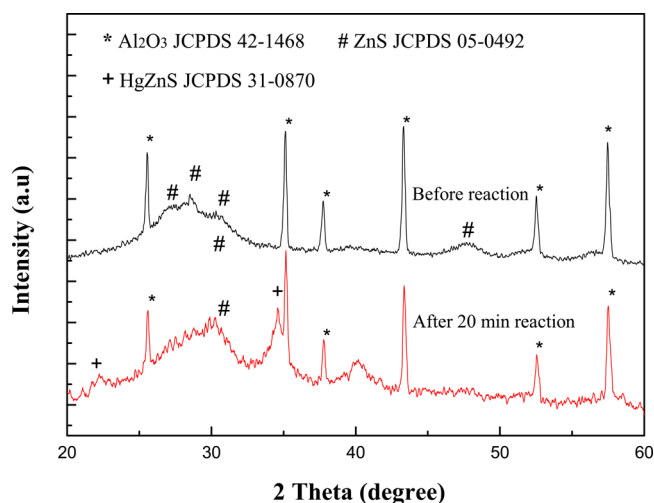
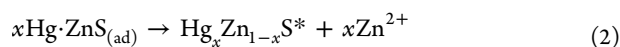
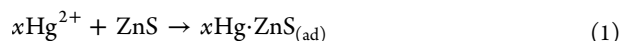


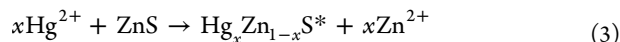
**Figure 4.** XRD patterns of ZnS NCs sorbents before and after mercury removal. ZnS NCs sorbent (L-3.0h) samples before reaction and after 20 min of reaction were analyzed by XRD, respectively.

$x\text{Hg}\cdot\text{ZnS}_{(\text{ad})}$  converted to an intermediate product,  $\text{Hg}_x\text{Zn}_{1-x}\text{S}^*$  and simultaneously released  $\text{Zn}^{2+}$ . In pathway 2, the  $\text{Hg}^{2+}$  directly reacted with ZnS NCs and formed  $\text{Hg}_x\text{Zn}_{1-x}\text{S}^*$  and released  $\text{Zn}^{2+}$  through the cation exchange reaction, and if the  $\text{Hg}^{2+}$  is in excess to  $\text{Zn}^{2+}$ , the  $\text{Hg}_x\text{Zn}_{1-x}\text{S}^*$  will finally turn to HgS. Equations 1–3 can be used to describe the reaction process.

Pathway 1



Pathway 2



Because the  $\text{Zn}^{2+}$  ions are exchanged with the same amount of  $\text{Hg}^{2+}$  ions eventually, the whole reaction between  $\text{Hg}^{2+}$  and ZnS NCs sorbent belongs to cation exchange.

### 3.4. Influence of pH Value and Other Metal Cations on Mercury Removal.

The pH value of industrial wastewater often varies with industry types, so it is important to investigate the influence of pH value on the  $\text{Hg}^{2+}$  removal efficiency. 100 mg of ZnS NCs sorbent (L-0.5h) was added into 50 mL of  $\text{HgCl}_2$  solution with stirring (400 r/min). The initial  $\text{Hg}^{2+}$  concentration is 297.5 mg/L (ppm). A certain amount of HCl solution was added into the  $\text{HgCl}_2$  solution to adjust its pH value from 1 to 6.

As shown in Figure 5, the  $\text{Hg}^{2+}$  removal efficiency is over 99.9% when the pH value is from 1 to 6. Obviously, the pH value will not affect the  $\text{Hg}^{2+}$  removal efficiency by ZnS NCs sorbent. It is well-known that ZnS is not stable at low pH conditions. We tried to mix the ZnS NCs sorbent with HCl solutions at different pH values. It was found that the ZnS NCs sorbent produced bubbles in low pH solutions and the  $\text{Zn}^{2+}$  concentration increased significantly with the decrease of the pH value (Table S1, Supporting Information). However, negligible  $\text{Zn}^{2+}$  could be detected when the pH value is from 4 to 6. That indicates that the ZnS NCs sorbent is stable when the pH value is from 4 to 6. Therefore, the reaction process of  $\text{Hg}^{2+}$  and ZnS NCs is different when the pH value is less than 3. There may be a third possible reaction pathway for  $\text{Hg}^{2+}$

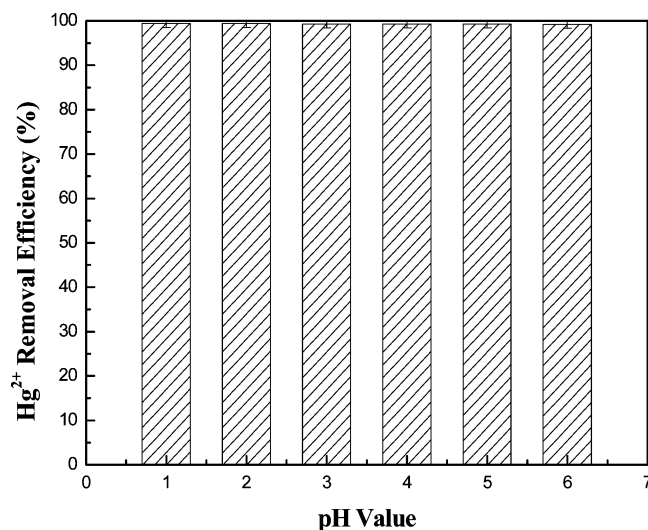
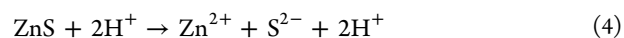


**Figure 5.** Influence of pH value on the  $\text{Hg}^{2+}$  removal efficiency. 100 mg of ZnS NCs (L-0.5h) sorbent was added into 50 mL of  $\text{HgCl}_2$  solution with stirring (400 r/min). The initial  $\text{Hg}^{2+}$  concentration is 297.5 mg/L (ppm). A certain amount of HCl solution was added into the  $\text{HgCl}_2$  solution to adjust its pH value from 1 to 6. The pH value of  $\text{HgCl}_2$  solution (297.5 mg/L) is about 5.5.

removal by ZnS NCs, which could be deduced as follows. First, part of the ZnS NCs dissolved in solution and formed  $\text{S}^{2-}$  or  $\text{H}_2\text{S}$  immediately when its pH value was less than 3. Then, the  $\text{S}^{2-}$  or  $\text{H}_2\text{S}$  reacted with  $\text{Hg}^{2+}$  and generated HgS. Finally, the produced HgS was adsorbed by the sorbent. Equations 4–8 can be used to describe the reaction process.

Pathway 3



In addition, several metal compounds, such as  $\text{CuSO}_4$ ,  $\text{Pb}(\text{NO}_3)_2$ ,  $\text{Ni}(\text{NO}_3)_2$ ,  $\text{Co}(\text{NO}_3)_2$ ,  $\text{CaCl}_2$ ,  $\text{CdCl}_2$  and  $\text{CrCl}_3$ , were added into the  $\text{HgCl}_2$  solution respectively to investigate the influence of other metal cations on  $\text{Hg}^{2+}$  removal by ZnS NCs sorbents (Figure S5, Supporting Information). According to Figure S5 (Supporting Information), the  $\text{Hg}^{2+}$  removal efficiency is still over 99.9%, even in the presence of other metal cations in 5 min. There is no obvious influence of other metal cations on the  $\text{Hg}^{2+}$  removal efficiency by the ZnS NCs sorbent. It may be because HgS has the smallest Ksp (solubility product constant) among the sulfides formed by the above metals. However, the presence of  $\text{Cu}^{2+}$  did slow the removal speed of  $\text{Hg}^{2+}$ . Meanwhile, the removal efficiencies of  $\text{Cu}^{2+}$ ,  $\text{Ni}^{2+}$ ,  $\text{Pb}^{2+}$  and  $\text{Cd}^{2+}$  were about 95%, 77%, 75% and 50%, respectively.

**3.5. Thickness-Dependent Cation Exchange.** To reveal how the thickness of the ZnS NCs layer affects the  $\text{Hg}^{2+}$  removal performance of sorbents, four samples with different thickness were tested (Figure 6). Because the saturated adsorption capacity of ZnS NCs sorbent for  $\text{Hg}^{2+}$  is very large, high mercury concentration simulated wastewater was

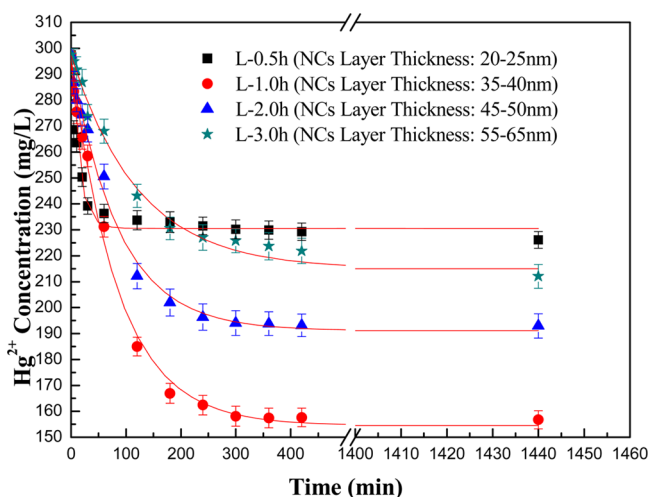


**Figure 6.** Influence of ZnS NCs layer thickness on  $\text{Hg}^{2+}$  removal. 20 mg of ZnS NCs adsorbent was mixed with 100 mL of  $\text{HgCl}_2$  solution ( $\text{Hg}^{2+}$  concentration: 297.5 mg/L) with stirring (400 r/min), where the  $\text{Hg}^{2+}$  is highly excessive to the ZnS NCs contained in the four sorbents. The pH value of  $\text{HgCl}_2$  solution (297.5 mg/L) is about 5.5.

tested in this research for saving the experimental time. 20 mg of ZnS NCs adsorbent was mixed with 100 mL of  $\text{HgCl}_2$  solution ( $\text{Hg}^{2+}$  concentration: 297.5 mg/L) with stirring (400 r/min), where the  $\text{Hg}^{2+}$  is highly excessive to the ZnS NCs contained in the four sorbents.

From Figure 6, we can see that the cation exchange reaction is faster when the ZnS NCs layer thickness is thinner, which can be explained by a simple scaling of the size in diffusion-controlled reaction schemes, where the reaction time is roughly proportional to the square of the size.<sup>12</sup> It also could be seen that the  $\text{Hg}^{2+}$  concentration decreases remarkably with the increasing contact time. The  $\text{Hg}^{2+}$  concentration of the solution treated by L-0.5h quickly reached a constant value in a short time, whereas the others took about 300 min to reach equilibrium. The final  $\text{Hg}^{2+}$  removal efficiency is about 24.0%, 47.3%, 35.1% and 28.7% for L-0.5h, L-1.0h, L-2.0h and L-3.0h, respectively.

The ZnS NCs sorbents component ratio (weight percent) before and after  $\text{Hg}^{2+}$  removal reaction were analyzed by EDX and inductively coupled plasma mass spectrometry (ICP-MS) (Table 2). Because the L-0.5h sorbent contains much less ZnS NCs than other three sorbents, its mercury removal efficiency of L-0.5h is the lowest of the four sorbents. Interestingly, L-1.0h

**Table 2.** Components Percentage (wt %) of ZnS NCs Sorbents before and after  $\text{Hg}^{2+}$  Removal Reaction Calculated by EDX and ICP-MS Analysis

reaction time	ZnS NCs	$\text{Al}_2\text{O}_3$	ZnS	HgS	$\eta^a$
before reaction	L-0.5h	81.4	18.6	0	0
	L-1.0h	64.1	35.9	0	0
	L-2.0h	53.1	46.9	0	0
	L-3.0h	51.3	48.7	0	0
after reaction	L-0.5h	69.1	0.1	30.8	99.4
	L-1.0h	46.4	1.0	52.6	96.2
	L-2.0h	41.1	17.2	41.7	52.6
	L-3.0h	40.6	25.9	33.5	32.8

<sup>a</sup> $\eta$  presents the exchange degree of  $\text{Zn}^{2+}$  of the ZnS NCs sorbents (at %).

has the best removal efficiency, even though its ZnS NCs component ratio is less than those of L-2.0h and L-3.0h. Table 2 shows that about 99.4%  $\text{Zn}^{2+}$  of L-0.5h and 96.2%  $\text{Zn}^{2+}$  of L-1.0h was exchanged by  $\text{Hg}^{2+}$ . However, only 32.8%  $\text{Zn}^{2+}$  of L-3.0h was exchanged by  $\text{Hg}^{2+}$  in the same solution. Obviously, the exchange capability of  $\text{Zn}^{2+}$  by  $\text{Hg}^{2+}$  is thickness dependent. The samples with thicker ZnS NCs layer were partially cation exchanged if the ZnS NCs layer thickness beyond a certain value (Figure S6, Supporting Information). Therefore, to control a suitable thickness of the exchange layer is very important for a good cation exchanger, which should have a compromise between exchange speed and adsorption capacity.

**3.6. Size-Dependent Cation Exchange.** Due to the similar ZnS NCs sizes of the four samples synthesized at 180 °C, their different cation exchange behaviors mentioned above should be mostly related to their thickness differences of the ZnS NCs layer. Does the size of the ZnS NCs affect the cation exchange? To answer this question, bigger sizes of ZnS NCs sorbents were synthesized at a higher temperature (270 °C). The ZnS NCs synthesized at 270 °C were marked as H-0.5h, H-1.0h, H-2.0h and H-3.0h, respectively. TEM images (Figure S7, Supporting Information) show H-0.5h has a similar thickness ZnS layer (20–25 nm) as that of L-0.5h but is composed with bigger ZnS NCs of 7–8 nm, and H-3.0h has a similar thickness (about 55–65 nm) as L-3.0h but with bigger ZnS NCs of about 17–18 nm. Then five samples contained ZnS particles of various sizes were tested to investigate the size-dependent behavior during the cation exchange. 20 mg of adsorbent was mixed with 100 mL of  $\text{HgCl}_2$  solution ( $\text{Hg}^{2+}$  concentration: 297.5 mg/L) with stirring (400 r/min).

As shown in Figure 7, the samples synthesized at a higher temperature with the same reaction time show slower cation

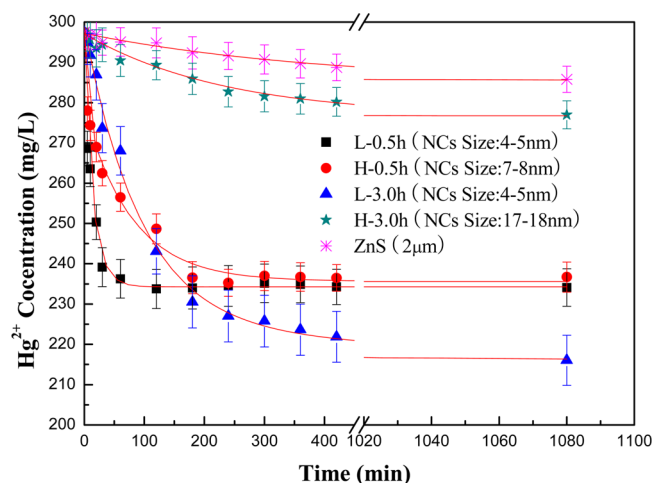


**Figure 7.** Size effects of ZnS NCs on  $\text{Hg}^{2+}$  removal. 20 mg of ZnS NCs adsorbent was mixed with 100 mL of  $\text{HgCl}_2$  solution ( $\text{Hg}^{2+}$  concentration: 297.5 mg/L) with stirring (400 r/min). The pH value of the  $\text{HgCl}_2$  solution (297.5 mg/L) is about 5.5.

exchange speeds. Particularly, the H-3.0h speed is much slower than the others and that for the 2  $\mu\text{m}$  ZnS particles is even worse. In this experiment, the differences of cation exchange speed should be attributed to the different sizes of the ZnS particles. Even with a similar layer thickness, a bigger ZnS NCs coating layer is more difficult to be exchanged. But interestingly, H-0.5h has a similar exchange capacity as L-0.5h, even though their sizes are different; it is possibly because

its ZnS NCs layer is thin enough to be completely exchanged by  $\text{Hg}^{2+}$ . These observations clearly demonstrate the intrinsic size effects of cation exchange in ZnS NCs, and further confirmed that the cation exchange between ZnS and  $\text{Hg}^{2+}$  was diffusion-limited. For ZnS NCs with bigger sizes, perhaps only part of the  $\text{Zn}^{2+}$  was exchanged by  $\text{Hg}^{2+}$  due to shallow diffusion depth and slow kinetics, which is similar to the observation in the cation exchange between thick CdS nanowires and  $\text{Zn}^{2+}$  in vapor-phase reaction at low temperature.<sup>27</sup>

**3.7. Influence of Initial  $\text{Hg}^{2+}$  Concentration on the Saturated Adsorption Capacity of ZnS NCs Sorbent.** The saturated adsorption capacity of the ZnS NCs sorbent for  $\text{Hg}^{2+}$  was measured at the initial  $\text{Hg}^{2+}$  concentration of 90.7–451.7 mg/L. To ensure that the adsorption equilibrium was reached, the samples were tested after a 24 h adsorption experiment. The saturated adsorption capacity of L-1.0h for  $\text{Hg}^{2+}$  is about 720 mg/g with the  $\text{Hg}^{2+}$  concentration range from 90.7 to 451.7 mg/L (Figure S8, Supporting Information). The initial  $\text{Hg}^{2+}$  concentration does not affect the saturated adsorption capacity of the ZnS NCs sorbent. If calculated by ZnS NCs themselves, the adsorption capacity is about 2000 mg/g, which is close to the theoretic saturated adsorption capacity and is much higher than those of recently reported mercury sorbents, such as a gold NCs adsorbent (676 mg/g),<sup>28</sup> Zn-doped biomagnetite particles (416 mg/g),<sup>29</sup> manganese dioxide nanowhiskers (199.5 mg/g),<sup>30</sup> functionalized diatom silica microparticles (185.2 mg/g)<sup>31</sup> and  $\text{Fe}_3\text{O}_4$  magnetic NCs with humic acid (97.7 mg/g).<sup>32</sup>

**3.8. Recycling of the Sorbent and Mercury.** The disposal of sorbents after use is important for a good sorbent, which should avoid causing a second pollution. It is well-known that HgS can dissolve into a high concentration  $\text{Na}_2\text{S}$  solution because of the formation of mercury polysulfide. A black sorbent after  $\text{Hg}^{2+}$  absorption was treated by  $\text{Na}_2\text{S}$  solution (1 M/L) and it turned to white in seconds (Figure S9, Supporting Information). Chemical analysis demonstrates that the white powder contains only 0.07% mercury. It means most of HgS formed by cation exchange dissolved into sodium sulfide, and the resulted concentrated mercury solution is easy to be recycled. The cleaned  $\text{Al}_2\text{O}_3$  nanoparticles could be reused for growing ZnS NCs again. Therefore, the ZnS NCs sorbent is a promising sorbent for mercury removal from industrial contaminated water.

## 4. CONCLUSIONS

To conclude, we report a novel efficient mercury scavenger based on ZnS NCs, which can remove over 99.9%  $\text{Hg}^{2+}$  in 1 min, and lower the  $\text{Hg}^{2+}$  concentration from 297.5 mg/L (ppm) to below 1.0  $\mu\text{g/L}$  (ppb) within 5 min. The saturated adsorption capacity of ZnS NCs themselves is about 2000 mg/g, which is close to the theoretic saturated adsorption capacity. We demonstrated the size and thickness dependent cation exchange between ZnS NCs and  $\text{Hg}^{2+}$ , and found the cation exchange will be difficult for ZnS NCs bigger than 17–18 nm, or a ZnS NCs layer thicker than 40 nm. Therefore, the ability to precisely control the scale of nanoparticles or layers is critical to synthesize a suitable heavy metal ions sorbent via cation exchange.

## ■ ASSOCIATED CONTENT

### Supporting Information

TEM images of  $\text{Al}_2\text{O}_3$  nanoparticles, EDX spectra of ZnS NCs sorbent, HRTEM images of L-0.5h and L-3.0h samples, color change of the ZnS NCs sorbent with the increase of the reaction time, influence of other cations on  $\text{Hg}^{2+}$  removal by ZnS NCs sorbent, illustration of thickness-dependent cation exchange of ZnS NCs sorbents during the reaction, TEM and HRTEM images of the samples synthesized at different temperature and corresponding XRD patterns, saturated adsorption capacity of ZnS NCs sorbent (L-1.0h) for  $\text{Hg}^{2+}$  in different initial  $\text{Hg}^{2+}$  concentrations, recycling experiment of the ZnS NCs sorbent after  $\text{Hg}^{2+}$  removal, and  $\text{Zn}^{2+}$  concentration of solution at the pH values from 1 to 6. This material is available free of charge via the Internet at <http://pubs.acs.org>.

## ■ AUTHOR INFORMATION

### Corresponding Authors

\*L. Li. Tel: +86 21 54745591. Fax: +86 21 54745591. E-mail: [liangli117@sjtu.edu.cn](mailto:liangli117@sjtu.edu.cn).

\*N.Q. Yan. Tel: +86 21 54745591. Fax: +86 21 54745591. E-mail: [nqyan@sjtu.edu.cn](mailto:nqyan@sjtu.edu.cn).

### Notes

The authors declare no competing financial interest.

## ■ ACKNOWLEDGMENTS

This study is supported by the National Basic Research Program of China (973 Program) (No. 2013CB430005), the National Natural Science Foundation of China (NSFC 21271179, 51278294), Program for New Century Excellent Talents (NCET-13-0364) and the National High Technology Research and Development Program (No. 2012AA062504). We thank Professor J. M. Pietryga from Los Alamos National Lab and Professor J. C. Ren from Shanghai Jiao Tong University for valuable discussions.

## ■ REFERENCES

- (1) Tchounwou, P. B.; Ayensu, W. K.; Ninashvili, N.; Sutton, D. Review: Environmental Exposure to Mercury and Its Toxicopathologic Implications for Public Health. *Environ. Toxicol.* **2003**, *18*, 149–175.
- (2) Mackey, T. K.; Contreras, J. T.; Liang, B. A. The Minamata Convention on Mercury: Attempting to Address the Global Controversy of Dental Amalgam Use and Mercury Waste Disposal. *Sci. Total Environ.* **2014**, *472*, 125–129.
- (3) Jarup, L. Hazards of Heavy Metal Contamination. *Br. Med. Bull.* **2003**, *68*, 167–182.
- (4) Jaiswal, A.; Ghosh, S. S.; Chattopadhyay, A. Quantum Dot Impregnated-Chitosan Film for Heavy Metal Ion Sensing and Removal. *Langmuir* **2012**, *28*, 15687–15696.
- (5) Dave, N.; Chan, M. Y.; Huang, P. J.; Smith, B. D.; Liu, J. W. Regenerable DNA-functionalized Hydrogels for Ultrasensitive, Instrument-Free Mercury (II) Detection and Removal in Water. *J. Am. Chem. Soc.* **2010**, *132*, 12668–12673.
- (6) Huttenloch, P.; Roehl, K. E.; Czurda, K. Use of Copper Shavings to Remove Mercury from Contaminated Groundwater or Wastewater by Amalgamation. *Environ. Sci. Technol.* **2003**, *37*, 4269–4273.
- (7) Ojea-Jimenez, I.; Lopez, X.; Arbiol, J.; Puentes, V. Citrate-coated Gold Nanoparticles as Smart Scavengers for Mercury (II) Removal from Polluted Waters. *ACS Nano* **2012**, *6*, 2253–2260.
- (8) Kumari, S.; Chauhan, G. S. New Cellulose-Lysine Schiff-Base-based Sensor-Adsorbent for Mercury Ions. *ACS Appl. Mater. Interfaces* **2014**, *6*, 5908–5917.



- (9) Parham, H.; Zargar, B.; Shiralipour, R. Fast and Efficient Removal of Mercury from Water Samples Using Magnetic Iron Oxide Nanoparticles Modified with 2-Mercaptobenzothiazole. *J. Hazard. Mater.* **2012**, *205–206*, 94–100.
- (10) Alivisatos, A. P. Semiconductor Clusters, Nanocrystals, and Quantum Dots. *Science* **1996**, *271*, 933–937.
- (11) Gupta, S.; Kershaw, S. V.; Rogach, A. L. Ion Exchange in Colloidal Nanocrystal. *Adv. Mater.* **2013**, *25*, 6923–6944.
- (12) Huang, D. W.; Niu, C. G.; Ruan, M.; Wang, X. Y.; Zeng, G. M.; Deng, C. H. Highly Sensitive Strategy for  $\text{Hg}^{2+}$  Detection in Environmental Water Samples Using Long Lifetime Fluorescence Quantum Dots and Gold Nanoparticles. *Environ. Sci. Technol.* **2013**, *47*, 4392–4398.
- (13) Luther, J. M.; Zheng, H.; Sadtler, B.; Alivisatos, A. P. Synthesis of Pb Nanorods and Other Ionic Nanocrystals with Complex Morphology by Sequential Cation Exchange Reactions. *J. Am. Chem. Soc.* **2009**, *131*, 16851–16857.
- (14) Smith, A. M.; Nie, S. Bright and Compact Alloyed Quantum Dots with Broadly Tunable Near-Infrared Absorption and Fluorescence Spectra through Mercury Cation Exchange. *J. Am. Chem. Soc.* **2011**, *133*, 24–26.
- (15) Dloczik, L.; Konenkamp, R. Nanostructure Transfer in Semiconductors by Ion Exchange. *Nano Lett.* **2003**, *3*, 651–653.
- (16) Son, D. H.; Hughes, S. M.; Yin, Y. D.; Alivisatos, A. P. Cation Exchange Reactions in Ionic Nanocrystals. *Science* **2004**, *306*, 1009–1012.
- (17) Cavallotti, R.; Goniakowski, J.; Lazzari, R.; Jupille, J.; Koltsov, A.; Loison, D. Role of Surface Hydroxyl Groups on Zinc Adsorption Characteristics on  $\alpha\text{-Al}_2\text{O}_3$  (0001) Surfaces: First-Principles Study. *J. Phys. Chem. C* **2014**, *118*, 13578–13589.
- (18) Lodziana, Z.; Nørskov, J. K. Adsorption of Cu and Pd on  $\alpha\text{-Al}_2\text{O}_3$  (0001) surfaces with different stoichiometries. *J. Chem. Phys.* **2001**, *115*, 11261–11267.
- (19) Wagner-Dobler, I. Pilot Plant for Bioremediation of Mercury Containing Industrial Waste Water. *Appl. Microbiol. Biotechnol.* **2003**, *62*, 124–133.
- (20) Reiss, P.; Protiere, M.; Li, L. Core/Shell Semiconductor Nanocrystals. *Small* **2009**, *5*, 154–168.
- (21) Li, L.; Pandey, A.; Werder, D. J.; Khanal, B. P.; Pietryga, J. M.; Klimov, V. I. Efficient Synthesis of Highly Luminescent Copper Indium Sulfide-based Core/Shell Nanocrystals with Surprisingly Long-Lived Emission. *J. Am. Chem. Soc.* **2011**, *133*, 1176–1179.
- (22) World Health Organization. *Guidelines for Drinking-water Quality*, 4<sup>th</sup> ed; World Health Organization: Geneva, Switzerland, 2011.
- (23) Pala, I. R.; Brock, S. L. ZnS Nanoparticle Gels for Remediation of  $\text{Pb}^{2+}$  and  $\text{Hg}^{2+}$  Polluted Water. *ACS Appl. Mater. Interfaces* **2012**, *4*, 2160–2167.
- (24) European Union.. Council Directive 98/83/EC on the Quality of Water Intended for Human Consumption. *Off. J. Eur. Communities: Legis.* **1998**, *41*, L 330/32–L 330/54.
- (25) Lou, Y. B.; Zhao, Y. X.; Chen, J. X.; Zhu, J. J. Metal Ions Optical Sensing by Semiconductor Quantum Dots. *J. Mater. Chem. C* **2014**, *2*, 595–613.
- (26) Duan, J. L.; Jiang, X. C.; Ni, S. Q.; Yang, M.; Zhan, J. H. Facile Synthesis of N-Acetyl-L-Cysteine Capped ZnS Quantum Dots as an Eco-Friendly Fluorescence Sensor for  $\text{Hg}^{2+}$ . *Talanta* **2011**, *85*, 1738–1743.
- (27) Zhang, B.; Jung, Y.; Chung, H. S.; Vugt, L. V.; Agarwal, R. Nanowire Transformation by Size-Dependent Cation Exchange Reactions. *Nano Lett.* **2010**, *10*, 149–155.
- (28) Lo, S. I.; Chen, P. C.; Huang, C. C.; Chang, H. T. Gold Nanoparticle-Aluminum Oxide Adsorbent for Efficient Removal of Mercury Species from Natural Waters. *Environ. Sci. Technol.* **2012**, *46*, 2724–2730.
- (29) He, F.; Wang, W.; Moon, J. W.; Howe, J.; Pierce, E. M.; Liang, L. Y. Rapid Removal of Hg (II) from Aqueous Solutions Using Thiolfunctionalized Zn-Doped Biomagnetite Particles. *ACS Appl. Mater. Interfaces* **2012**, *4*, 4373–4379.
- (30) Lisha, K. P.; Maliyekkal, S. M.; Pradeep, T. Manganese Dioxide Nanowhiskers: A Potential Adsorbent for the Removal of Hg (II) from Water. *Chem. Eng. J.* **2010**, *160*, 432–439.
- (31) Yu, Y.; Mensah, J. A.; Losic, D. Functionalized Diatom Silica Microparticles for Removal of Mercury Ions. *Sci. Technol. Adv. Mater.* **2012**, *13*, 1–11.
- (32) Liu, J. F.; Zhao, Z. S.; Jiang, G. B. Coating  $\text{Fe}_3\text{O}_4$  Magnetic Nanoparticles with Humic Acid for High Efficient Removal of Heavy Metal in Water. *Environ. Sci. Technol.* **2008**, *42*, 6949–6954.